Mutations in *C10orf11*, a Melanocyte-Differentiation Gene, Cause Autosomal-Recessive Albinism

Karen Grønskov,[1,5,10,*] Christopher M. Dooley,[2,10] Elsebet Østergaard,[3] Robert N. Kelsh,[4] Lars Hansen,[5] Mitchell P. Levesque,[6] Kaj Vilhelmsen,[7] Kjeld Møllgård,[5] Derek L. Stemple,[2] and Thomas Rosenberg[8,9]

Autosomal-recessive albinism is a hypopigmentation disorder with a broad phenotypic range. A substantial fraction of individuals with albinism remain genetically unresolved, and it has been hypothesized that more genes are to be identified. By using homozygosity mapping of an inbred Faroese family, we identified a 3.5 Mb homozygous region (10q22.2–q22.3) on chromosome 10. The region contains five protein-coding genes, and sequencing of one of these, *C10orf11*, revealed a nonsense mutation that segregated with the disease and showed a recessive inheritance pattern. Investigation of additional albinism-affected individuals from the Faroe Islands revealed that five out of eight unrelated affected persons had the nonsense mutation in *C10orf11*. Screening of a cohort of autosomal-recessive-albinism-affected individuals residing in Denmark showed a homozygous 1 bp duplication in *C10orf11* in an individual originating from Lithuania. Immunohistochemistry showed localization of C10orf11 in melanoblasts and melanocytes in human fetal tissue, but no localization was seen in retinal pigment epithelial cells. Knockdown of the zebrafish (*Danio rerio*) homolog with the use of morpholinos resulted in substantially decreased pigmentation and a reduction of the apparent number of pigmented melanocytes. The morphant phenotype was rescued by wild-type *C10orf11*, but not by mutant *C10orf11*. In conclusion, we have identified a melanocyte-differentiation gene, *C10orf11*, which when mutated causes autosomal-recessive albinism in humans.

Autosomal-recessive albinism (oculocutaneous albinism [OCA (MIM 203100)]) is the most common condition among hypopigmentation disorders.[1] The disease is genetically heterogeneous and can be caused by mutations in at least four genes; however, a substantial fraction of individuals with albinism remain genetically unresolved.[2]

Melanin-producing cells originate from two lineages of progenitor cells: the outer neuroepithelium of the optic cup and the neural crest. Melanocyte development includes fate specification, migration, and differentiation in a temporally and spatially tightly controlled process.[3,4] Melanogenesis involves a complex, but still only partially characterized, gene regulatory network.[5–11]

The four OCA types are distinguished on the basis of clinical and molecular findings. OCA type 1 (MIM 203100 and 606952) and OCA type 3 (MIM 203290) are directly involved in melanin synthesis through *TYR* (MIM 606933)-encoded tyrosinase and *TYRP1* (MIM 115501)-encoded tyrosinase-related protein 1. OCA type 2 (MIM 203200) is caused by mutations in *OCA2* (MIM 611409), encoding a melanosomal membrane protein, and OCA type 4 (MIM 606574) is due to mutations in *SLC45A2* (MIM 606202), encoding a melanosomal membrane-associated transporter protein. Still, unknown genes are thought to be involved in this disorder.

Fifteen individuals with autosomal-recessive albinism were examined at the outpatient eye clinic at the National Hospital in Tórshavn, Faroe Islands, and six of these were also examined at least once at the National Eye Clinic for the Visually Impaired, Denmark. The assessments consisted of a routine ophthalmological examination including motility, refraction, best Snellen visual acuity, slit lamp with transillumination, and ophthalmoscopy. Furthermore, Goldmann visual-field measurements, fundus photography, electroretinography, visual-evoked potentials (VEPs) with monocular and binocular flash and checkerboard stimulation, and bioccipital recording for the measurement of crossed asymmetry of the visual pathways were performed on eight affected persons. In one individual, ocular coherence tomography (OCT) of the macular region was performed.

The study followed the guidelines of the Helsinki Declaration and was approved by the local ethics committee and by the Scientific Ethical Committee of the Faroe Islands, and it was contracted with the Biobank under the Faroese Ministry of Health. Affected individuals and healthy relatives were informed of the nature of the study, and written informed consent was obtained from all participants.

Homozygosity mapping was performed with the Affymetrix SNP6.0 platform (Affymetrix, Santa Clara, CA, USA). The analysis was performed by AROS Applied Biotechnology A/S (Århus, Denmark). CNCHP files were generated with Genotyping Console (version 4.0) and

[1]Applied Human Molecular Genetics, Kennedy Center, Copenhagen University Hospital, Rigshospitalet, DK-2100 Copenhagen, Denmark; [2]Mouse and Zebrafish Genetics, Wellcome Trust Sanger Institute, Wellcome Trust Genome Campus, Hinxton, Cambridge, CB10 1SA, UK; [3]Department of Clinical Genetics 4062, Copenhagen University Hospital, Rigshospitalet, DK-2100 Copenhagen, Denmark; [4]Department of Biology & Biochemistry and Centre for Regenerative Medicine, University of Bath, Bath BA2 7AY, UK; [5]Department of Cellular and Molecular Medicine, University of Copenhagen, DK-2200 Copenhagen, Denmark; [6]Department of Dermatology, University of Zurich Hospital, CH-8006 Zurich, Switzerland; [7]Department of Ophthalmology, National Hospital of the Faroe Islands, FO-100 Tórshavn, the Faroe Islands; [8]National Eye Clinic for the Visually Impaired, Kennedy Center, Copenhagen University Hospital, Rigshospitalet, DK-2100 Copenhagen, Denmark; [9]Gordon Norrie Center for Genetic Eye Diseases, DK-2400 Copenhagen, Denmark
[10]These authors contributed equally to this study
*Correspondence: karen.groenskov@regionh.dk
http://dx.doi.org/10.1016/j.ajhg.2013.01.006.

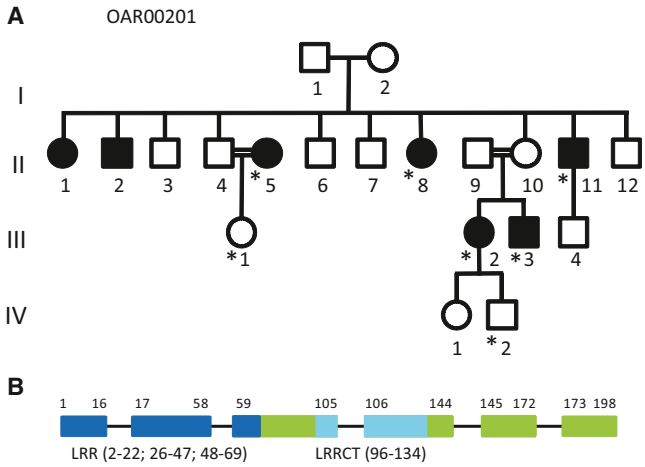

Figure 1. Homozygosity Mapping
(A) Pedigree of family OAR00201. Filled symbols are individuals affected by OCA, and open symbols are unaffected individuals. Individual II5 is a second-degree cousin of II4, and individual II9 is a second-degree cousin of II10. Individuals II5 and II9 are also second-degree cousins. Individuals used for homozygosity mapping are marked with an asterisk.
(B) Genomic structure of *C10orf11*. Boxes are exons, and the numbers above the boxes are amino acid numbers. Dark-blue areas are leucine-rich repeat (LRR) domains, and light-blue areas are the LRR C-terminal (LRRCT) domains (numbers in brackets are amino acid numbers).

analyzed by Chromosome Analysis Suite (version 1.2.2) software (Affymetrix) with default settings (minimum ten markers; loss of heterozygosity minimum physical size of 1 Mb). Five affected members from family OAR00201 were used for the initial analysis (Figure 1A). In addition, two unaffected family members were included for subtraction of nonrelevant homozygous regions. This revealed one homozygous region on chromosome 10 (chr10: 77,233,812–80,685,953; UCSC Genome Browser hg19). Three additional affected individuals (two sisters and one isolated case) were found to be homozygous in an overlapping region (Figure S1, available online).

The region contains five protein-coding RefSeq genes: *C10orf11* (MIM 614537), *KCNMA1* (MIM 600150), *DLG5* (MIM 604090), *POLR3A* (MIM 614258), and *RPS24* (MIM 602412) (Figure S2). Furthermore, two genes (*LOC100128292* and *LOC100132987*) encoding noncoding RNA molecules were located in the region. Mutations in *KCNMA1* are a known cause of generalized epilepsy and paroxysmal dyskinesia (MIM 609446).[12] Mice with knockout of both *Dlg5* alleles show renal cysts and hydrocephalus.[13] *POLR3A* encodes the largest and catalytic core component of RNA polymerase III, and mutations in *POLR3A* are known to cause leukodystrophy, hypomyelinating, 7, with or without oligodontia and/or hypogonadotropic hypogonadism (MIM 607694). Mutations in *RPS24*, encoding a ribosomal protein, are known to cause Diamond-blackfan anemia 3 (MIM 610629). Mutations in either of these genes seemed unlikely to cause albinism.

We therefore started out by sequencing *C10orf11* (primers are listed in Table S1). This revealed a homozygous nonsense mutation, c.580C>T (p.Arg194*) (RefSeq accession number NM_032024.3), in all five affected individuals from family OAR00201. Analysis of a further eight unrelated affected individuals revealed five with the same mutation. This means that in nine families with autosomal-recessive albinism, probands from six of them were shown to have the nonsense mutation in *C10orf11*. Probands from the nine Faroese families had been previously analyzed in some or all of *TYR*, *OCA2*, *SLC45A2*, and *TYRP1* (Table S2).The six families with the nonsense mutation were shown to share a common ancestor in both the paternal and maternal lines. Analysis of eight unaffected relatives from four families showed segregation in accordance with autosomal-recessive inheritance. Ninety-two control individuals from the Faroe Islands were analyzed by high-resolution melting analysis. In brief, a PCR product of 105 bp was amplified with primers 5′-GAAGTGTCGCTACGTTTACTATGG-3′ and 5′-TTCATGAAATGGGTGAAGGT-3′. Amplification products were analyzed in a 96-well LightScanner instrument (HR96, Biofire, Salt Lake City, UT, USA), and melting data were collected in the temperature range of 60°C –98°C. Data were analyzed with LightScanner software with Call-IT (version 2.0, Biofire). Three individuals were carriers of c.580C>T, corresponding to a carrier frequency of 3.3%.

We next considered whether mutations in *C10orf11* are a cause of autosomal-recessive albinism in other populations. Forty-eight genetically unexplained individuals who had autosomal-recessive albinism and who were residing in Denmark were screened for mutations in *C10orf11*. Of these, 42 had previously been screened for mutations in *TYR*, *OCA2*, *TYRP1*, and *SLC45A2* (21 had no obvious mutations, 13 had one *TYR* mutation, 7 had one *OCA2* mutation, and 1 had one *TYR* mutation and one *OCA2* mutation),[2] whereas the remaining six persons had no prior investigation. In one individual, we found a mutation in *C10orf11*. This person (individual 76121), originating from Lithuania, was apparently homozygous for a 1 bp duplication (c.66dupC [p.Ala23Argfs*39]); however, a deletion on one allele cannot be ruled out and neither can a preferential amplification of one allele because of a sequence variation on the second allele (although primers were checked by the SNPCheck program for minimizing this risk). The possibility of a second mutation in linkage disequilibrium with the *C10orf11* mutations contributing to the phenotype also cannot be ruled out.

Most of the affected individuals had a light Northern complexion with a tendency to lighter pigmentation than that of their relatives. Eye symptoms were predominant: nystagmus and iris transillumination were present in all subjects. The phenotypic characteristics of nine affected individuals are shown in Table 1. Extremely sparse pigmentation of the peripheral ocular fundus was seen (Figure 2). Visual acuity varied between 6/9 and 3/60.

Table 1. Clinical Signs and Symptoms in Nine Individuals with Homozygous *C10orf11* Mutations

Individual ID	Mutation	Snellen Visual Acuity	Refraction	Iris Transillumination	Scalp Hair Color	Misrouting	Miscellaneous
PN0224	c.[580C>T];[580C>T]	R 6/60 L 6/60	R +6.50 −2.00 × 0° L +6.00 −1.00 × 10°	extensive	blond with reddish tint	ND	esotropia 25° in R eye
PN0220	c.[580C>T];[580C>T]	R 6/36 L 6/36	R +6.50 −2.00 × 160° L +6.50 −2.00 × 30°	extensive	blond	+	esotropia 15° in L eye
PN0278	c.[580C>T];[580C>T]	R 6/18 L 6/18	R +1.50 −3.00 × 0° L +1.50 −3.00 × 0°	extensive	dark brown	+	dark brown eyebrows and lashes, slow tanning
PN0207	c.[580C>T];[580C>T]	R 6/30 L 6/24	R +3.00 −3.50 × 15° L +3.00 −3.00 × 165°	extensive	blond	+	none
PN0302	c.[580C>T];[580C>T]	R 3/60 L 3/60	R +0.50 −2.00 × 10° L +0.50 −2.00 × 10°	only peripheral	blond	+	cone-rod dystrophy,[a] blond eyebrows and lashes
PN0303	c.[580C>T];[580C>T]	R 6/30 L 6/30	L +5.00 −1.50 × 130° L +7.00 −1.50 × 130°	extensive	blond	+	cone-rod dystrophy[a]
PN0295	c.[580C>T];[(580C>T)]	R 3/60 L 3/60	R +7.50 −3.50 × 20° L +7.50 −3.00 × 15°	extensive	white	+	exotropia in R eye
PN0449	c.[580C>T];[(580C>T)]	R 6/36 L 6/36	R +5.00 −1.00 × 170° L +4.50 −1.50 × 20°	extensive	dark blond	+	none
76121	c.[66dupC];[(66dupC)]	R 6/30 L 6/30	R +2.25 −3.00 × 175° L +2.50 −3.00 × 5°	extensive	dark blond	+	corneal surgery (Moscow, 1982)

Individuals whose ID number begins with "PN" belong to the population of the Faroe Islands. Individuals PN0224 (III2) and PN0220 (II8) belong to the index pedigree. Individuals PN0278, PN0207, PN0295, and PN0449 stated to have no affected relatives. Individual 76121 was born in Lithuania by Lithuanian parents. None of the individuals showed signs of Wardenburg syndrome, i.e., white forelock, premature graying of the hair, dystopia canthorum, hypopigmented or hyperpigmented areas of skin, craniofacial dysmorphism, or sensineural deafness. The following abbreviations are used: R, right; L, left; and ND, no data.
[a]PN0302 and PN0303 are sisters and, in addition to the *C10orf11* mutation, had a deleterious homozygous *PCDH21* mutation causing cone-rod dystrophy.[14]

VEP recordings showed crossed asymmetry of the cortical visual response in all tested individuals (n = 8). Photophobia was not a major problem. Hair color varied from pale blond to dark brown.

C10orf11 encodes a 198 amino acid protein containing three leucine-rich repeats (LRRs) and one LRR C-terminal (LRRCT) domain (Figure 1B). LRRs containing proteins cover a broad spectrum of functions and include cell adhesion and signaling, extracellular-matrix assembly, platelet aggregation, neuronal development, RNA processing, and immune response.[15]

The localization of C10orf11 in human tissue specimens was investigated in samples of human embryonic and fetal eye and skin tissues. These were obtained either from the archives of the Department of Cellular and Molecular Medicine at the University of Copenhagen or from legal abortions performed at the Department of Obstetrics and Gynecology, Frederiksberg Hospital. Oral and written information was given, and informed consent was obtained from all contributing women and was approved by the Regional Committee on Biomedical Research Ethics of Copenhagen and Frederiksberg (KF (01) 258206). Samples from the adult human eye were also included. Late in the human embryonic period, neural crest cells migrate into the mesenchyme of the developing dermis, where they differentiate into C10orf11-positive melanocyte precursors (melanoblasts) (Figures 3A and 3B). Later, the majority migrate to the dermoepidermal junction, penetrate the basal membrane, and differentiate into strongly stained melanocytes in the basal layer of epidermis and in hair follicles (Figure 3C). All control sections were negative (Figure S3). Parallel sections that included retinal pigment epithelium (RPE) in the developing human eye showed no reactivity to C10orf11 (Figure S4). This localization pattern is consistent with a gene that is important for and acts cell autonomously in melanocyte differentiation and function.

To advance our understanding of the function of *C10orf11*, we employed the zebrafish (*Danio rerio*) as a model organism. Zebrafish embryos were obtained via natural spawning essentially as described.[16] Replicates of morpholino experiments were carried out in WIK, TLF, and SAT zebrafish backgrounds. A single zebrafish homolog, *c10orf11*, is known and shows 69% similarity at both the nucleotide and amino acid levels (Figure 4A). mRNA expression was investigated by in situ hybridization, which was essentially carried out as previously stated (Zebrafish Model Organism Database). Oligonucleotides (*c10orf11* and *c10orf11_T7*) (Table S3) were designed for generating a *c10orf11* PCR product. Antisense probes were synthesized from the PCR products with the use of digoxigenin-labeled nucleotide triphosphates and T7 polymerase. Sense probes were produced in a similar manner and were used for negative controls. Expression of *c10orf11* was seen in migrating neural crest cells (Figures 4B–4D). This suggests that *c10orf11* might have a conserved role in pigment cell development in zebrafish. To test whether

Figure 2. Fundus Pictures
(Upper left) Right eye of individual PN0278.
(Upper right) Right eye of individual PN0207.
(Lower left) Right eye of individual 76221. All fundi show indistinct foveal regions and a lack of reflexes and extremely reduced pigmentation of the choroid in the periphery.
(Lower right) An OCT scan through the foveal region of the right eye of individual 76221 shows foveal hypoplasia (aplasia) and complete absence of the foveal depression.

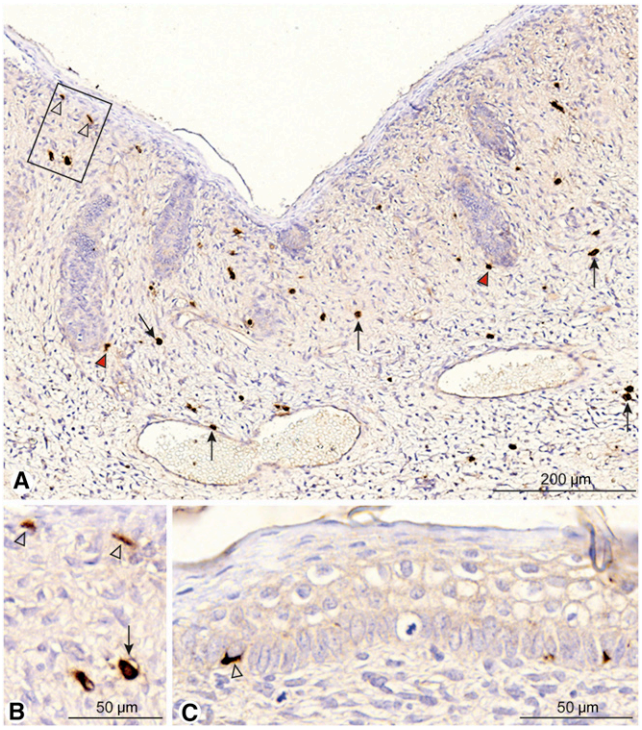

Figure 3. Localization of C10orf11 in Human Fetal Tissue
Immunocytochemical detection of C10orf11 in skin from the lower lip of a 14-week-old human fetus. The tissue was fixed in 4% buffered formalin or Bouin's fixative for at least 18 hr and subsequently embedded in paraffin. Serial sections, 4 mm thick, were cut and placed on silanized slides. Immunohistochemistry was performed by deparaffinized sections in xylene and then rehydrated in a series of graded alcohols, treated with a 0.5% solution of hydrogen peroxide in methanol for 15 min for quenching endogenous peroxidase, and then rinsed in Tris-buffered saline (TBS) (5 mm Tris-HCl, 146 mm NaCl, pH 7.6). Nonspecific binding was inhibited by incubation for 30 min with 2% casein (C-7078, Sigma, St. Louis, MO, USA) at room temperature. The sections were then incubated overnight at 4°C first with a polyclonal goat antibody against C10orf11 (P-18) ([sc-241949] from Santa Cruz Biotechnology [Santa Cruz, CA, USA]) diluted 1:100 in 2% casein and then with anti-sheep/goat Ig (biotinylated whole antibody [from donkey, RPN1025V] [GE Healthcare, Uppsala, Sweden]) diluted 1:20 in casein for 30 min at room temperature. Finally, sections were incubated with VECTASTAIN R.T.U. Elite ABC Reagent (PK-7100 from Vector Laboratories, Burlingame, CA, USA) for 30 min at room temperature. The sections were washed with TBS and then incubated for 6 min with DAB chromogen solution, counterstained with Mayers hematoxylin, dehydrated in graded alcohols followed by xylene, and coverslipped with DPX mounting medium (Merck, Darmstadt, Germany).
(A and B) Numerous melanocyte precursors (some indicated by arrows) show strong reactivity in dermis. A few are in contact with hair bulbs (red arrowheads) (A). The framed area is shown in higher magnification in (B), where melanocyte precursors are in contact with the basal membrane of the dermoepidermal junction (open arrowheads). The scale bars in (A) and (B) represent 200 μm and 50 μm, respectively.
(C) From the same specimen, a melanocyte precursor has migrated into the basal layer of the epidermis (open arrowhead) and differentiated into a melanocyte. The scale bar represents 50 μm.

the expressing cells included melanoblasts, we examined *c10orf11* expression in *mitfa* mutant embryos. Mitfa is required for specification, maintenance, and differentiation of the melanocyte lineage.[17] In contrast to wild-type siblings, *mitfa*^{w2} mutants[18] showed highly reduced *c10orf11* expression and no detectable expression in migrating neural crest cells, clearly consistent with expression in melanoblasts. Residual expression in cells that we interpret as premigratory neural crest cells (Figures 4E and 4F, arrowheads) indicates that expression might be initially induced by a *mitfa*-independent mechanism.

These data encouraged us to explore a role for *c10orf11* in melanocyte development by knockdown with morpholino antisense oligonucleotides (MOs) (Figures 4G and 4H). Three morpholinos were designed to specifically knockdown zebrafish *c10orf11* (ENSDART00000145499): ATG-MO[19] to block any transcript including potential maternal transcript, Ex-skip MO to block splicing, and Int_Ret_MO[20] to block zygotic transcripts. We also incorporated the use of the Tp53 MO and a standard control morpholino when stated. See Table S3 for sequences of morpholinos. The Tp53 MO was used to decrease apoptosis triggered by nonspecific morpholino-induced Tp53 activation.[21] All morpholinos were produced by GeneTools (Philomath, OR, USA). To control the efficacy of the splice-blocking Ex-skip MO, we performed RT-PCR on cDNA (Transcriptor High Fidelity cDNA Synthesis Kit, Roche, Basel, Switzerland) generated from 24 hpf (hours postfertilization) morphant embryos by using oligonucleotides ex2F and ex2R (Table S3). It was possible to confirm a splice skipping of exon 2 via RT-PCR band shift (Figure 4I). We focused on the early pigment cell phenotype because morphant larvae were observed to go into developmental

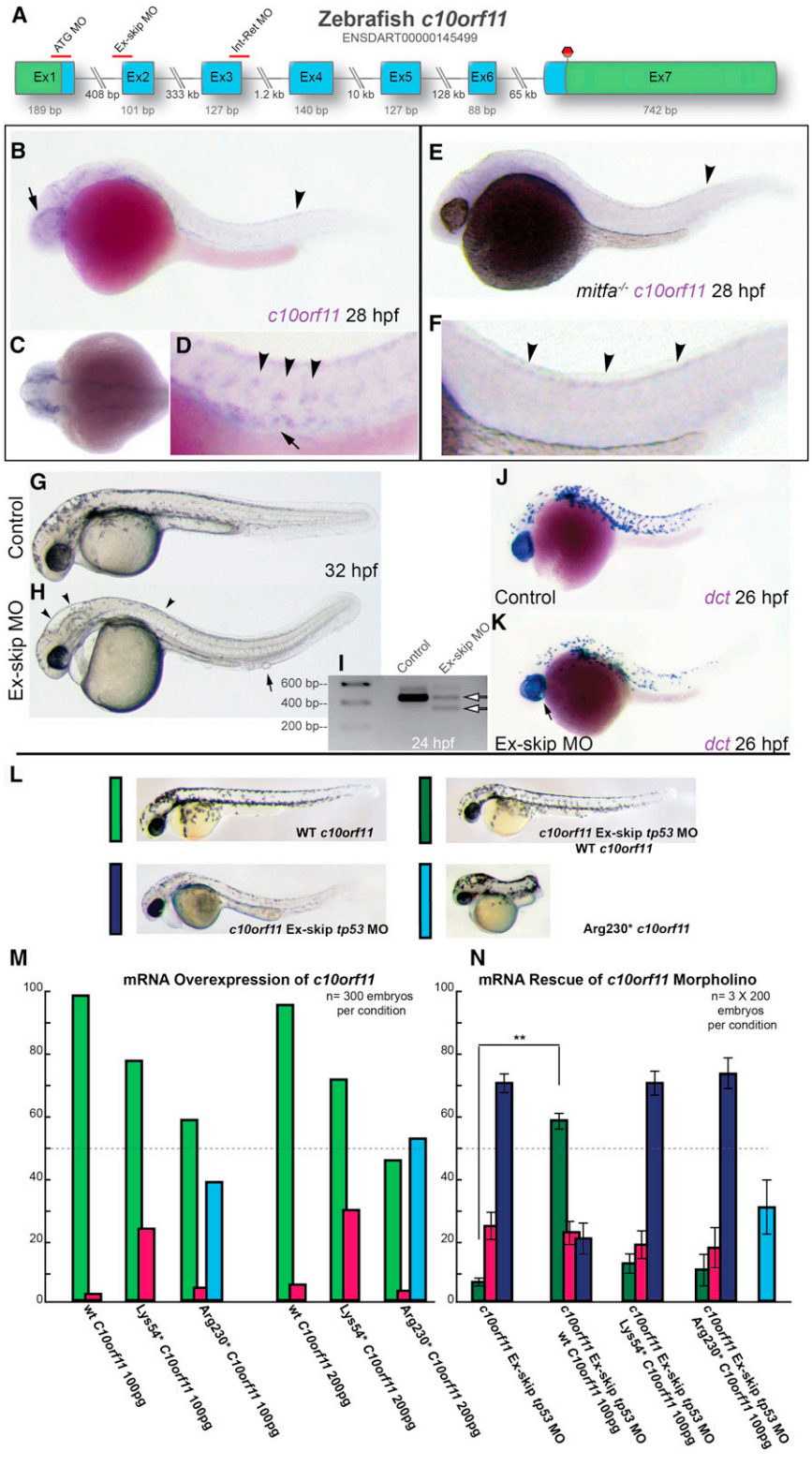

Figure 4. Zebrafish Developmental Expression and Morpholino Knockdown of *c10orf11*

(A) The transcript structure and length of *c10orf11* is displayed with all seven exons. The coding sequence is in blue, and the UTR is in green. The relative positions of the three characterized morpholinos are also shown.

(B) In situ expression of *c10orf11* at 28 hpf can be detected in the migrating neural crest cells of the cranium and trunk (arrowhead).

(C) Enlargement of dorsal view shows cranial neural crest migrating around the eye toward the optic stalk and oral ectoderm.

(D) Expression of *c10orf11* in neural crest (arrowheads) paths and around the dorsal aorta (arrow).

(E) In situ expression of *c10orf11* at 28 hpf in *mitfa*$^{-/-}$ mutant embryos. Some residual expression is seen (arrowheads).

(F) Enlargement of dorsal view.

(G and H) A mixture of scrambled morpholino (5 ng) and Tp53 (6 ng) was used in control morphants (G) and Ex-skip MO (5 ng) + Tp53 MO (6 ng) (H) knockdowns. Morphants were raised under standard conditions, and their morphology was observed over the next 72 hr of development. In morphants, a strong reduction in melanocyte number along the dorsal axis (arrowheads), as well as blistering of the epidermis (arrow) and a failure of melanocytes to migrate over the yolk sac, can be seen.

(I) Partial targeted knockdown of the *c10orf11* transcript with Ex-skip MO is shown by a 101 bp band shift between control and morphant cDNA in an RT-PCR assay. Morphants show both the normal endogenous transcript (larger band) and the morpholino missplicing event causing the skipping of *c10orf11* exon 2 (lower band) on a DNA gel.

(J and K) *c10orf11* morphants present a partial reduction of *dct* expression and the number of *dct*-positive melanoblasts at 26 hpf.

(L) Capped mRNA was transcribed and injected at the 1-cell stage alone or with the *c10orf11* Ex2 splice MO, giving rise to a range of phenotypes. The colored bars to the left of the images correspond to the bars in the charts in (M) and (N). The magenta-colored bars represent embryos that failed to develop properly beyond 8 hpf.

(M) Injections of wild-type *c10orf11* mRNA and truncated versions p.Lys54* and p.Arg230* at two concentrations. Overexpression of p.Arg230* mRNA led to a consistent axis shortening and a notochord defect that was absent from the wild-type and p.Lys54* injections.

(N) Only the wild-type mRNA of *c10orf11* significantly rescued the morphant phenotype (dark-green bar, two-sample t test, $p < 0.010$). *C10orf11* Ex-skip tp53 MO- and p.Arg230*-injected embryos also failed to rescue morphant phenotypes, but about a third of total embryos (light-blue bar) presented with the ectopic phenotype of p.Arg230*. The error bars express the SEM based on three repetitions of 200 injections.

arrest at 48–72 hpf. Melanization of the RPE was first seen at 24 hpf in wild-type animals and was followed by the melanization of the neural-crest-derived melanocytes soon after; by 32 hpf, melanocytes migrated away from the dorsal neural tube and were dispersed throughout most of the head, anterior trunk, and yolk sac (Figure 4G). In the morphants, there was a strong reduction in the apparent number of pigmented melanocytes, and the remaining cells showed substantially decreased pigmentation (Figure 4H). Epidermal blistering along ventral and dorsal fin folds was also prominent among most morphants at this stage (Figure 4H). Similar phenotypic results were obtained with ATG-MO, as well as when ATG-MO and Ex-skip MO were mixed at half concentrations (data not shown).

To test whether melanoblasts are present but not pigmented, we performed in situ hybridization with the melanoblast-specific marker dopachrome tautomerase (*dct* [MIM 191275]) at 26 hpf by using a probe generated with the primers *dct* and *dct_T7* (Table S3 and Figures 4J and 4K). This showed a partial reduction in both *dct* expression levels and the apparent melanoblast number in the *c10orf11* morphants, indicating that *c10orf11* is important for multiple aspects of melanocyte development, including differentiation. However, MO knockdown of *c10orf11* in zebrafish did not completely abolish pigmented melanocytes. This is consistent with the phenotype observed in the human probands, who showed some pigmentation in hair and skin. Furthermore, some residual endogenous expression of *c10orf11* was observed in the embryos (Figure 4I). To complement our knockdown studies, we then cloned the full-length zebrafish *c10orf11* cDNA into the pGEMT cloning vector (Promega, Madison, WI, USA) by using primers 5′-CGTCAGTGGGAGTCTT CGT-3′ and 5′-CTCGCGTGTCTATCCACTGA-3′ on zebrafish cDNA from 24 hpf embryos. The *c10orf11* cDNA was then subcloned by restriction digestion with EcoRI and then by T4-DNA ligation into the PCS2+ expression vector. Clones with the correct orientation and no coding mutations were identified by sequencing. We then created two truncated versions, p.Lys54* and p.Arg230* (Figure S5), mimicking the alterations identified in humans. We generated capped *c10orf11* mRNA (SP6 message-machine, Life Technologies, Paisley, UK) of all three forms and then carried out a series of injections into zebrafish embryos at the 1-cell stage. All three *c10orf11* mRNAs were injected at titrated concentrations for the establishment of an effective concentration (data not shown). When injected at two different amounts (100 pg and 200 pg per embryo), wild-type *c10orf11* mRNA failed to give obvious ectopic phenotypes, whereas embryos injected with p.Arg230* were dwarfed and lacked a notochord in about half the cases (Figure 4M). The *c10orf11* Ex-skip MO was coinjected with wild-type *c10orf11*, p.Lys54*, or p.Arg230* for testing the ability to rescue the morphant phenotype (Figure 4L). When the same *c10orf11* mRNAs were coinjected with Ex-skip MO, the wild-type mRNA, unlike truncated versions p.Lys54* and p.Arg230*, was able to significantly rescue the morphant phenotype ($p < 0.010$) (Figure 4N).

Currently, the likely biological function of *C10orf11* remains poorly understood. Studies by Wada and collaborators show that an homolog of human *C10orf11* is involved in beta-catenin (MIM 116806) signaling in early *Ciona intestinalis* embryos and suggest that *C10orf11* functions upstream of or parallel to beta-catenin.[22] The Wnt/beta-catenin pathway plays an important role in fundamental biological processes involving cellular adhesion, tissue morphogenesis, and oncogenesis.[23] Beta-catenin has been shown to be required for melanocyte specification and has the transcription-factor-encoding *Mitfa* or *MITF* (MIM 156845) as a downstream target,[24–26] perhaps suggesting that *C10orf11* might function upstream of *MITF*. However, our preliminary zebrafish results showing decreased expression of *c10orf11* in *mitfa* mutants indicate that *c10orf11* expression lies downstream of *mitfa*. *MITF* plays a critical role in the development of specific cell types, including neural-crest-derived melanocytes and optic-cup-derived RPE cells, and furthermore functions as a master regulator of melanocyte development, including the regulation of all core enzymes necessary for melanin biogenesis, such as tyrosinase, tyrosinase-related protein 1, and dopachrome tautomerase.[27] Mutations in *MITF* cause Waardenburg syndrome (type 2A [MIM 193510]) and show an autosomal-dominant inheritance. Waardenburg syndromes are auditory-pigmentary disorders characterized by congenital sensorineural hearing loss and pigmentary disturbances of iris, hair, and skin. We would expect that mutations in a gene functioning upstream of *MITF* would cause a more severe phenotype than OCA. More experiments are needed for determining the position of *C10orf11* in the melanogenesis gene regulatory network. Because the precise relationship between *MITF* and *C10orf11* in melanocyte development and differentiation is still an area of ongoing study, the reason that the affected individuals have an albino phenotype is not completely clear at this time.

In conclusion, we have identified mutations in a melanocyte-differentiation gene, *C10orf11*, in individuals with autosomal-recessive albinism. Mutational analysis of *C10orf11* in larger cohorts of individuals with albinism is needed for estimating the contribution of this gene to these diseases.

Supplemental Data

Supplemental Data include five figures and three tables and can be found with this article online at http://www.cell.com/AJHG.

Acknowledgments

The study was supported by a grant from The Danish Association of the Blind. We thank Søren Petersen, Alma Dedic, Pia Skovgaard, and Jette Bune Rasmussen (Kennedy Center, Copenhagen University Hospital, Rigshospitalet) for technical assistance. We would

also like to thank Hans-Martian Maischein of the Nuesslein-Volhard lab for sending us mitfaw2 embryos. The expert technical assistance of Hanne Hadberg and Pernille S. Froh (Department of Cellular and Molecular Medicine, Faculty of Health Sciences, University of Copenhagen) is gratefully acknowledged.

Received: August 25, 2012
Revised: October 17, 2012
Accepted: January 23, 2013
Published: February 7, 2013

Web Resources

The URLs for data presented herein are as follows:

ExonPrimer, http://ihg.gsf.de/ihg/ExonPrimer.html
Human Genome Variation Society, http://www.hgvs.org/mutnomen/
Online Mendelian Inheritance in Man (OMIM), http://www.omim.org
RefSeq, http://www.ncbi.nlm.nih.gov/RefSeq
SNPCheck, https://ngrl.manchester.ac.uk/SNPCheckV3/snpcheck.htm
UCSC Genome Browser, http://genome.ucsc.edu/
Zebrafish Model Organism Database, http://zfin.org

References

1. Tomita, Y., and Suzuki, T. (2004). Genetics of pigmentary disorders. Am. J. Med. Genet. C. Semin. Med. Genet. *131C*, 75–81.
2. Grønskov, K., Ek, J., Sand, A., Scheller, R., Bygum, A., Brixen, K., Brondum-Nielsen, K., and Rosenberg, T. (2009). Birth prevalence and mutation spectrum in danish patients with autosomal recessive albinism. Invest. Ophthalmol. Vis. Sci. *50*, 1058–1064.
3. Sommer, L. (2011). Generation of melanocytes from neural crest cells. Pigment Cell Melanoma Res. *24*, 411–421.
4. Murisier, F., and Beermann, F. (2006). Genetics of pigment cells: Lessons from the tyrosinase gene family. Histol. Histopathol. *21*, 567–578.
5. Dupin, E., Calloni, G.W., and Le Douarin, N.M. (2010). The cephalic neural crest of amniote vertebrates is composed of a large majority of precursors endowed with neural, melanocytic, chondrogenic and osteogenic potentialities. Cell Cycle *9*, 238–249.
6. Greenhill, E.R., Rocco, A., Vibert, L., Nikaido, M., and Kelsh, R.N. (2011). An iterative genetic and dynamical modelling approach identifies novel features of the gene regulatory network underlying melanocyte development. PLoS Genet. *7*, e1002265.
7. Hou, L., and Pavan, W.J. (2008). Transcriptional and signaling regulation in neural crest stem cell-derived melanocyte development: Do all roads lead to Mitf? Cell Res. *18*, 1163–1176.
8. Lang, D., Lu, M.M., Huang, L., Engleka, K.A., Zhang, M., Chu, E.Y., Lipner, S., Skoultchi, A., Millar, S.E., and Epstein, J.A. (2005). Pax3 functions at a nodal point in melanocyte stem cell differentiation. Nature *433*, 884–887.
9. Loftus, S.K., Baxter, L.L., Buac, K., Watkins-Chow, D.E., Larson, D.M., and Pavan, W.J. (2009). Comparison of melanoblast expression patterns identifies distinct classes of genes. Pigment Cell Melanoma Res. *22*, 611–622.
10. Schiaffino, M.V. (2010). Signaling pathways in melanosome biogenesis and pathology. Int. J. Biochem. Cell Biol. *42*, 1094–1104.
11. Tachibana, M. (2000). MITF: A stream flowing for pigment cells. Pigment Cell Res. *13*, 230–240.
12. Du, W., Bautista, J.F., Yang, H., Diez-Sampedro, A., You, S.A., Wang, L., Kotagal, P., Lüders, H.O., Shi, J., Cui, J., et al. (2005). Calcium-sensitive potassium channelopathy in human epilepsy and paroxysmal movement disorder. Nat. Genet. *37*, 733–738.
13. Nechiporuk, T., Fernandez, T.E., and Vasioukhin, V. (2007). Failure of epithelial tube maintenance causes hydrocephalus and renal cysts in Dlg5-/- mice. Dev. Cell *13*, 338–350.
14. Ostergaard, E., Batbayli, M., Duno, M., Vilhelmsen, K., and Rosenberg, T. (2010). Mutations in PCDH21 cause autosomal recessive cone-rod dystrophy. J. Med. Genet. *47*, 665–669.
15. Bella, J., Hindle, K.L., McEwan, P.A., and Lovell, S.C. (2008). The leucine-rich repeat structure. Cell. Mol. Life Sci. *65*, 2307–2333.
16. Westerfield, M. (2000). The Zebrafish book. A guide for the laboratory use of zebrafish (Danio rerio), Fourth Edition (Eugene: University of Oregon Press).
17. Lister, J.A., Close, J., and Raible, D.W. (2001). Duplicate mitf genes in zebrafish: Complementary expression and conservation of melanogenic potential. Dev. Biol. *237*, 333–344.
18. Lister, J.A., Robertson, C.P., Lepage, T., Johnson, S.L., and Raible, D.W. (1999). nacre encodes a zebrafish microphthalmia-related protein that regulates neural-crest-derived pigment cell fate. Development *126*, 3757–3767.
19. Ekker, S.C. (2000). Morphants: A new systematic vertebrate functional genomics approach. Yeast *17*, 302–306.
20. Draper, B.W., Morcos, P.A., and Kimmel, C.B. (2001). Inhibition of zebrafish fgf8 pre-mRNA splicing with morpholino oligos: A quantifiable method for gene knockdown. Genesis *30*, 154–156.
21. Langheinrich, U., Hennen, E., Stott, G., and Vacun, G. (2002). Zebrafish as a model organism for the identification and characterization of drugs and genes affecting p53 signaling. Curr. Biol. *12*, 2023–2028.
22. Wada, S., Hamada, M., Kobayashi, K., and Satoh, N. (2008). Novel genes involved in canonical Wnt/beta-catenin signaling pathway in early Ciona intestinalis embryos. Dev. Growth Differ. *50*, 215–227.
23. Mulholland, D.J., Dedhar, S., Coetzee, G.A., and Nelson, C.C. (2005). Interaction of nuclear receptors with the Wnt/beta-catenin/Tcf signaling axis: Wnt you like to know? Endocr. Rev. *26*, 898–915.
24. Widlund, H.R., Horstmann, M.A., Price, E.R., Cui, J., Lessnick, S.L., Wu, M., He, X., and Fisher, D.E. (2002). Beta-catenin-induced melanoma growth requires the downstream target Microphthalmia-associated transcription factor. J. Cell Biol. *158*, 1079–1087.
25. Dorsky, R.I., Raible, D.W., and Moon, R.T. (2000). Direct regulation of nacre, a zebrafish MITF homolog required for pigment cell formation, by the Wnt pathway. Genes Dev. *14*, 158–162.
26. Hari, L., Brault, V., Kléber, M., Lee, H.Y., Ille, F., Leimeroth, R., Paratore, C., Suter, U., Kemler, R., and Sommer, L. (2002). Lineage-specific requirements of beta-catenin in neural crest development. J. Cell Biol. *159*, 867–880.
27. Wan, P., Hu, Y., and He, L. (2011). Regulation of melanocyte pivotal transcription factor MITF by some other transcription factors. Mol. Cell. Biochem. *354*, 241–246.